Journal of Solid State Chemistry **162,** 347–353 (2001)
doi:10.1006/jssc.2001.9381, available online at http://www.idealibrary.com on IDEAL®

Synthesis and Structures of a Layered and a Tubular Antimony(III) Phosphonate

Brian A. Adair,* Nathalie Guillou,† Marisol Alvarez,* Gérard Férey,† and Anthony K. Cheetham*,[1]

*Materials Research Laboratory, University of California, Santa Barbara, California 93106; and †Institut Lavoisier UMR CNRS 8637, Université de Versailles-St Quentin, 45 Avenue des Etats-Unis, 78035 Versailles Cedex, France

IN HONOR OF PROFESSOR PAUL HAGENMULLER ON THE OCCASION OF HIS 80TH BIRTHDAY

$Sb_2O(CH_3PO_3)_2$ (1) and $NH_4(SbO)_3(CH_3PO_3)_2$ (2) were synthesized by hydrothermal methods and their structures solved from powder and single-crystal X-ray diffraction data, respectively. 1 is monoclinic, space group $P2_1/c$ (No. 14) with $a = 4.7569(3)$ Å, $b = 19.944(1)$ Å, $c = 9.9147(5)$ Å, $\beta = 95.292(5)^\circ$, $V = 936.60(6)$ Å^3, $Z = 4$. 2 is triclinic, space group $P\bar{1}$ (No. 2) with $a = 6.915(2)$ Å, $b = 9.506(3)$ Å, $c = 9.800(3)$ Å, $\alpha = 105.254(5)^\circ$, $\beta = 94.206(5)^\circ$, $\gamma = 90.807(5)^\circ$, $V = 619.4(3)$ Å^3, $Z = 2$. Both structures contain 3-rings made from corner-sharing $[SbO_4E]$ and $[CH_3PO_3]$ polyhedra. 1 is a layered material, while 2 is a solid made of nanotubes containing building motifs related to the spiro-5 units found in some $[TO_4]$-based open frameworks.

Key Words: **hydrothermal synthesis; open-framework structures; phosphonate compounds.**

1. INTRODUCTION

Open frameworks based on antimony(III) have until recently included only thioantimonates (1) and the cetineite (2) family of chalcogenoantimonates, the latter containing $[Sb_{12}O_{18}]$ nanotubes. Both classes of materials are built from distorted $[SbX_3E]$ square pyramids, $[SbX_4E]$ trigonal bipyramids, and $[SbX_5E]$ octahedra [$X = 0$, S, Se; $E =$ lone pair], employing various combinations of primary ($r_{Sb-X} < 2.4$ Å), intermediate (2.4 Å $< r_{Sb-X} <$ 2.7 Å), and secondary (2.7 Å $< r_{Sb-X} <$ 3.1 Å) bonding. This variety of Sb^{III} coordination polyhedra, along with potential redox sites associated with lone pair $5s^2$ electrons, could give rise to unique properties in Sb^{III}-based materials. In fact, $K_3SbSe_3 \cdot 3Sb_2O_3$ is the first known photo- and semiconducting nanoporous material (3). The recently reported open-framework tin(II) phosphates (4), antimony(III) phosphates (5), and antimony(III) diphosphonates (6) have architectures that are quite different from those based on the ubiquitous four-connected tetrahedral nets found in zeolites and AlPOs (7). In keeping with this theme, we have looked to the monophosphonates of Sb^{III}, since four-coordinated/topologically three-connected RPO_3 tetrahedra impart both organic functionality and structural differences compared to the phosphates. We have discovered two closely related phases, one of which is constructed from Sb^{III} phosphonate nanotubes.

[1]To whom correspondence should be addressed. Fax: 805-893-8797. E-mail: cheetham@mrl.ucsb.edu.

2. EXPERIMENTAL

2.1. Synthesis of a Layered Antimony(III) Methyl Phosphonate, 1, $Sb_2O(CH_3PO_3)_2$

Polycrystalline samples of **1** can be made from a mixture of antimony(III) acetate, methylphosphonic acid, and water in a molar ratio of 1 Sb:1.1 P:250 H_2O. The mixture is sealed in a PTFE-lined stainless steel autoclave and heated at 135°C under autogenous pressure for 2 days. While **1** can be made in a variety of solvents, including ethanol, ethylene glycol, and dioxane, attempts to grow single crystals were unsuccessful.

2.2. Synthesis of a Tubular Antimony(III) Methyl Phosphonate, 2, $NH_4(SbO)_3(CH_3PO_3)_2$

The synthesis that resulted in the largest crystals of **2** was as follows: A mixture of antimony(III) acetate, methylphosphonic acid, urea, and ethanol (190 proof) in a molar ratio of 1 Sb:1.1 P:1.0 urea:10H_2O:80 EtOH was sealed in a PTFE-lined stainless steel autoclave and heated at 150°C under autogenous pressure for 2 days. The major product was **1**, but colorless crystals of **2** ($\sim 300 \times 80 \times 30$ μm) were isolated from the powder of **1** by floatation separation. In addition, crystals of Sb_2O_3 of about the same size and in about the same amount as **2** were present, so it is difficult to obtain large amounts of pure **2** with this synthesis. A synthesis that results in a powder form of nearly pure **2**, with small amounts of **1** and Sb_2O_3 (< 5%, as estimated by the relative heights of the largest peaks in the powder diffraction

0022-4596/01 $35.00

pattern), uses antimony(III) acetate, methylphosphonic acid, ammonium bicarbonate, and ethanol in a molar ratio of 1 Sb:0.75 P:1.4 NH_4^+:20 H_2O:150 EtOH at 150°C for 2 days. Substituting ethanol for ethylene glycol will also give **2**, but with considerably more **1** and Sb_2O_3 as impurities. Substituting ethylene glycol for water gives only Sb_2O_3. Using antimony(III) oxide as the starting reagent will give small amounts of **2** in ethanol (again, with **1** and Sb_2O_3 in the products) while attempts to form **2** in ethylene glycol were unsuccessful.

2.3. *Structure Determination of **1** from Powder X-Ray Diffraction*

X-ray powder diffraction data for **1** were collected on a Siemens D5000 diffractometer using Cu$K\alpha$ radiation ($\lambda = 1.5418$ Å). In order to avoid preferred orientation effects, hand-ground powder was side-loaded into the sample-holder. The powder diffraction pattern was scanned over an angular range of 3–100° (2θ) with a counting time of 45 s step^{-1}. An accurate determination of the peak positions and relative intensities for Cu$K\alpha_1$ radiation contributions was carried out with the software package DIFFRACT-AT. Pattern indexing was performed by means of the computer program DICVOL91 (8), using the 20 lowest angle reflections with an absolute error on peak positions of 0.03° (2θ). A monoclinic solution was found with satisfactory figures of merit [$M_{20} = 78$, $F_{20} = 170$ (0.0046, 38)]. The refined cell parameters were obtained from the complete data set and reviewed with the program NBS*AIDS83 (9). Systematic absences ($0k0$, $k = 2n + 1$ and $h0l$, $l = 2n + 1$) were consistent with the space group $P2_1/c$. Calculations were performed with the EXPO package (10), integrating EXTRA (11) for extracting integrated intensities and SIR*97* (12) for direct methods structure solution. All nonhydrogen atoms were found from the Fourier map with the highest figure of merit. The corresponding atomic coordinates were used as the starting model in the Rietveld refinement using the FULLPROF program (13) integrated in winPLOTR software (14). A pseudo-Voigt function was selected to describe individual line profiles. In order to describe the angular dependence of the peak width at half-maximum, the usual quadratic function in $\tan\theta$ was used. The final Rietveld refinement carried out in the angular range 7–99° (2θ) used 947 reflections. It involved the following parameters: 39 atomic coordinates; 4 common isotropic temperature factors adopted for Sb, P, O, and C atoms; 1 scale factor; 1 zero-point; 4 cell parameters; 3 half-width and 4 line asymmetry parameters; 2 variables for angular variation in η; and 6 polynomial background coefficients. Soft constraints were introduced for the PO_3CH_3 groups: d(P–O) = 1.50(2) Å and d(P–C) = 1.80(2) Å. Final agreement factors defined in Refs. (15) and (16) are $R_p = 0.088$, $R_{wp} = 0.113$ (profile factors), $R_B = 0.063$, $R_F = 0.027$ (crystal structure model indicators). Figure 1 shows the final fit obtained between calculated and observed patterns. The atomic coordinates and isotropic displacement parameters of **1** are given in Table 1 and selected bond distances and angles are listed in Table 2. Crystal data for **1**: space group $P2_1/c$ (No. 14), $a = 4.7569(3)$ Å, $b = 19.944(1)$ Å, $c = 9.9147(5)$ Å,

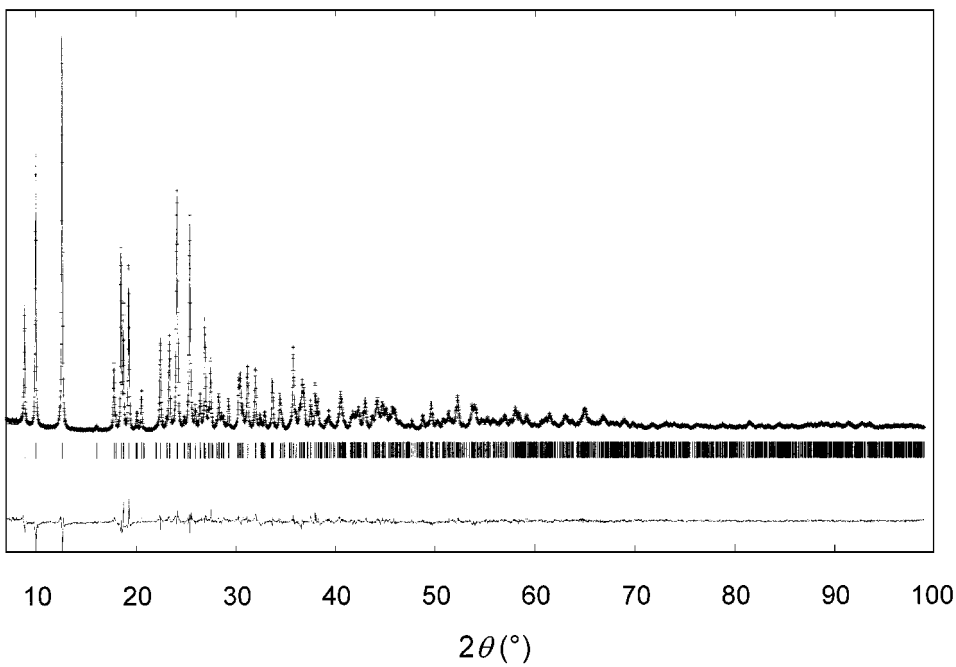

FIG. 1. Final Rietveld plot of calculated and observed X-ray powder patterns of **1**.

TABLE 1
Atomic Coordinates and Isotropic Displacement Parameters (Å²) for $Sb_2O(CH_3PO_3)_2$ (1)

Atom	*x*	*y*	*z*	*U*(iso)
Sb1	− 0.1661(6)	0.1081(1)	0.4675(3)	0.0045(9)Å²
Sb2	0.8135(6)	0.3152(1)	0.6535(3)	0.0045(9)Å²
P1	0.315(2)	0.1965(5)	0.6872(9)	0.0052(3)Å²
P2	0.244(2)	0.4515(5)	0.7399(9)	0.0052(3)Å²
O1	0.153(5)	0.263(1)	0.640(2)	0.02(3)Å²
O2	0.207(5)	0.143(1)	0.579(2)	0.02(3)Å²
O3	0.626(3)	0.209(1)	0.680(2)	0.02(3)Å²
O4	0.095(5)	0.451(1)	0.865(2)	0.02(3)Å²
O5	0.090(4)	0.409(1)	0.634(2)	0.02(3)Å²
O6	0.537(3)	0.432(1)	0.766(2)	0.02(3)Å²
O7	0.853(4)	0.176(1)	0.341(2)	0.02(3)Å²
C1	0.274(6)	0.165(1)	0.857(2)	0.003(8)Å²
C2	0.258(7)	0.531(1)	0.648(3)	0.003(8)Å²

$\beta = 95.292(5)^\circ$, $V = 936.60(6)$ Å^3, $Z = 4$, $M_w = 447.51$ g mol^{-1}, $D_c = 3.17$ g cm^{-3}.

2.4. *Structure Determination of* **2** *from Single-Crystal X-Ray Diffraction*

A single crystal of **2** was distinguished from crystals of Sb_2O_3 by its shape and glued to a thin glass fiber with cyanoacrylate (Superglue) adhesive. X-ray data were collected on a Bruker SMART CCD diffractometer equipped with a normal focus, 2.4 kW sealed tube X-ray source (Mo$K\alpha$ radiation, $\lambda = 0.71073$ Å) operating at 45 kV and 35 mA. A full sphere of intensity data was collected in 2252 frames with ω scans (width 0.30°, exposure time 10 s frame^{-1}). A total of 6409 reflections were collected in the range $-9 \le h \le 9$; $-12 \le k \le 12$; $-12 \le l \le 12$, and merged to give 2751 unique reflections ($R_{merg} = 0.0609$). An absorption correction was performed with the program SADABS (17). Unit cell constants were determined by a least-squares fit of 3807 reflections in the range $4.32^\circ < 2\theta < 56.60^\circ$ (18). Structural determination was achieved using SHELXS-97 and refinement against $|F|^2$ was carried out using the SHELXTL-PLUS package of programs (18). Hydrogen atoms were attached to carbon centers using a riding model. The last cycles of refinement included anisotropic thermal parameters for all nonhydrogen atoms. Final reliability factors are $R(F) = 0.0388$, $R_w(F^2) = 0.0804$ for all data with $S = 1.049$ (19). The final difference Fourier map has maximum and minimum peaks of 1.162 and − 1.371 e Å^{-3}, respectively. The atomic coordinates and equivalent isotropic displacement parameters of **2** are given in Table 3 and selected bond distances and angles are listed in Table 4. Crystal data for **2**: space group $P\bar{1}$ (No. 2), $a = 6.915(2)$ Å, $b = 9.506(3)$ Å, $c = 9.800(3)$ Å,

TABLE 2
Selected Bond Distances (Å) and Angles (°) for $Sb_2O(CH_3PO_3)_2$ (1)

	Distances	Angles
Sb1–O2	2.12(2)	
O4[a]	2.05(2)	86(1)
O6[b]	2.47(2)	157(2), 75(1)
O7[c]	1.85(2)	91(2), 91(2), 75(1)
Sb2–O1[d]	1.94(2)	
O3	2.32(2)	81(1)
O5[d]	2.31(2)	87(1), 168(2)
O7[e]	1.86(2)	96(2), 89(2), 90(1)
P1–O1	1.58(2)	
O2	1.56(2)	104(2)
O3	1.51(2)	107(2), 110(2)
C1	1.82(2)	118(2), 110(2), 107(2)
P2–O4	1.48(2)	
O5	1.49(2)	110(2)
O6	1.44(2)	112(2), 112(2)
C2	1.83(2)	117(2), 100(2), 104(2)

Symmetry transformations used to generate equivalent atoms: [a] $x, -y+\frac{1}{2}, z-\frac{1}{2}$; [b] $x-1, -y+\frac{1}{2}, z-\frac{1}{2}$; [c] $x-1, y, z$; [d] $x+1, y, z$; [e] $x, -y+\frac{1}{2}, z+\frac{1}{2}$.

TABLE 3
Atomic Coordinates and Equivalent Isotropic Displacement Parameters (Å²) for $NH_4(SbO)_3(CH_3PO_3)_2$ (2)

Atom	*x*	*y*	*z*	*U*(eq)
Sb1	0.07741(5)	0.26144(4)	0.82936(4)	0.01639(11)
Sb2	0.81565(5)	− 0.04867(4)	0.83138(4)	0.01714(11)
Sb3	0.20638(5)	0.32675(4)	0.50571(4)	0.01704(11)
P1	0.5459(2)	0.27539(15)	0.76688(16)	0.0170(3)
P2	0.1252(2)	0.68084(16)	0.76170(16)	0.0183(3)
O1	0.2858(6)	− 0.1766(4)	0.2231(5)	0.0224(9)
O2	0.4771(6)	0.2622(5)	0.6124(4)	0.0268(10)
O3	0.6225(6)	− 0.2388(5)	0.1528(4)	0.0240(9)
O4	0.1413(6)	0.5293(4)	0.7768(5)	0.0302(10)
O5	− 0.0779(6)	0.3132(5)	0.3930(4)	0.0246(9)
O6	− 0.9686(6)	0.2313(4)	0.1460(5)	0.0235(9)
O7	− 0.0589(5)	− 0.0473(4)	0.1908(4)	0.0194(8)
O8	0.0714(6)	0.2260(4)	0.6226(4)	0.0180(8)
O9	0.2577(6)	0.1389(4)	0.3694(4)	0.0218(9)
N1	0.7399(8)	0.0662(6)	0.4579(6)	0.0268(11)
C1	− 1.6322(9)	0.5427(7)	0.1526(9)	0.0352(17)
C2	− 0.3507(9)	0.2217(7)	0.1815(7)	0.0254(13)
H1A	− 1.5276	0.4774	0.1526	0.053
H1B	− 1.6821	0.5346	0.0567	0.053
H1C	− 17335	0.5179	0.2050	0.053
H2A	− 0.4447	0.2608	0.2476	0.038
H2B	− 0.3344	0.1205	0.1770	0.038
H2C	− 0.3947	0.2313	0.0893	0.038

Note. Hydrogen atoms were placed in calculated positions and held in a riding model; isotropic displacement parameters were chosen as 1.5 times that of the associated C center.

TABLE 4
Selected Bond Distances (Å) and Angles (°) for $NH_4(SbO)_3(CH_3PO_3)_2$ (2)

	Distances	Angles
Sb1–O8	1.962(4)	
O7[a]	1.994(4)	90.47(17)
O3[b]	2.088(4)	92.08(16), 85.73(16)
O1[a]	2.599(2)	83.74(15), 71.63(13), 156.89(15)
Sb2–O9[b]	1.954(4)	
O7[b]	1.955(4)	97.86(1)
O6[a]	2.099(4)	92.41(16), 89.85(16)
O1[b]	2.440(4)	84.65(15), 75.99(14), 164.96(15)
Sb3–O8	1.952(4)	
O9	1.983(4)	91.32(17)
O5	2.168(4)	82.99(16), 86.92(16)
O2	2.249(4)	84.55(16), 79.06(16), 160.99(16)
P1–O1[b]	1.520(4)	
O2	1.526(4)	110.9(2)
O3[b]	1.537(5)	110.5(2), 110.3(2)
C1[c]	1.775(6)	107.1(3), 108.8(3), 109.2(3)
P2–O4	1.491(4)	
O5[d]	1.544(4)	113.3(3)
O6[c]	1.568(4)	112.6(3), 107.9(2)
C2[d]	1.777(6)	109.7(3), 105.9(3), 107.0(3)

Symmetry transformations used to generate equivalent atoms: [a] $-x, -y, -z+1$; [b] $-x+1, -y, -z+1$; [c] $-x-1, -y+1, -z+1$; [d] $-x, -y+1, -z+1$.

$\alpha = 105.254(5)^\circ$, $\beta = 94.206(5)^\circ$, $\gamma = 90.807(5)^\circ$, $V = 619.4(3)$ Å^3, $Z = 2$, $M_w = 619.33$ g mol^{-1}, $D_c = 4.39$ g cm^{-3}.

2.5. Other

Elemental analysis of Sb and P was performed on a Thermo Jarrell Ash IRIS inductively coupled plasma (ICP) spectrometer. Thermogravimetic analysis (TGA) was performed on a Mettler STARe analyzer in air at a heating rate of 10°C min^{-1}. Product gases were analyzed by a coupled Balzers ThermoStar mass spectrometer.

3. RESULTS

3.1. Structure of *1*, $Sb_2O(CH_3PO_3)_2$

If we describe the local Sb^{III} environment in terms of the stereochemically active lone pair (E) plus the primary and intermediate Sb–O bonds ($r < 2.7$ Å), then the building units of **1** are two [SbO_4E] trigonal bipyramids and two [$MePO_3$] tetrahedra. These combine to form one type of "Sb_2P" 3-ring (made up of two [SbO_4E] and one [$MePO_3$] corner-sharing polyhedra); one Sb_3P_2 5-ring; and two Sb_3P_3 6-rings, one of which is made from edge-sharing

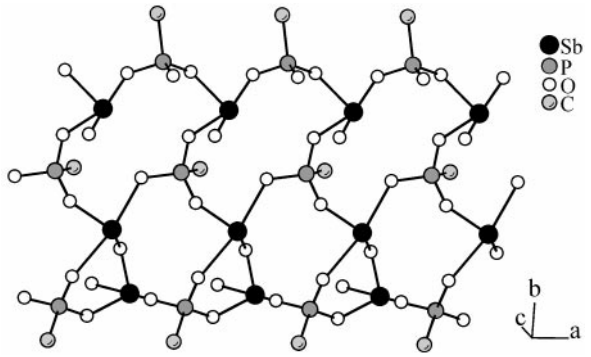

FIG. 2. The layers of **1** are made of Sb_2P, Sb_3P_2, and Sb_3P_3 rings.

3- and 5-rings (Fig. 2). These two types of 6-rings are linked together to form corrugated layers (Fig. 3a). Many of the framework metal *diphosphonates* are composed of inorganic layers bridged by diphosphonate groups, and it was previously noted that the framework of $Sb_2O(O_3PCH_2PO_3)$

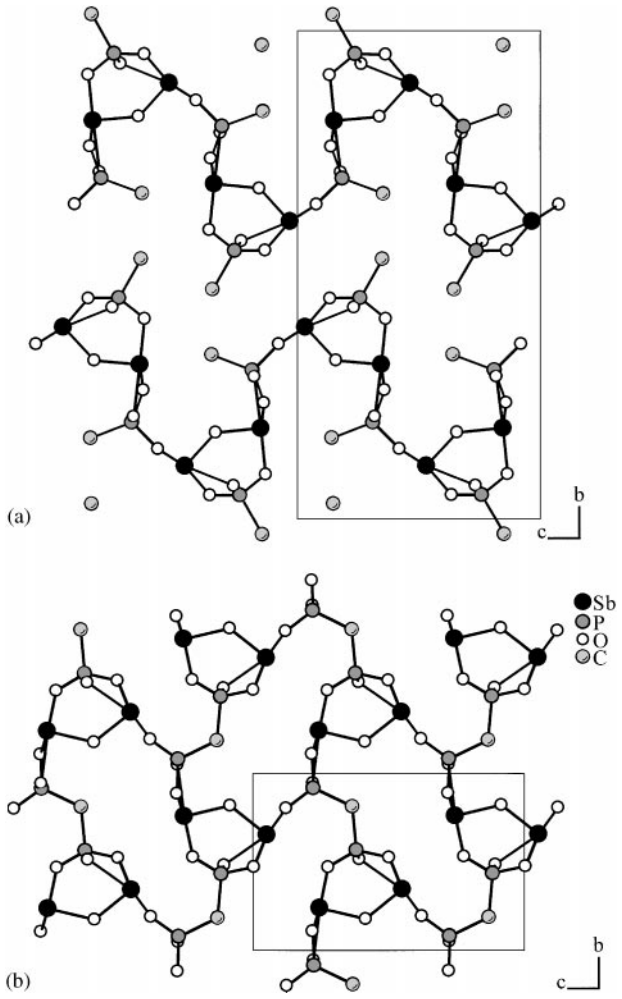

FIG. 3. The layers of (a) $Sb_2O(CH_3PO_3)$ (**1**) are like those found in (b) $Sb_2O(O_3PCH_2PO_3)$.

(Fig. 3b) consists of corrugated layers cross-linked through the methylene group of the diphosphonate (6). In fact, those layers are virtually identical to the layers of **1**, where the methylene group of the framework structure has been replaced by a terminal methyl group in **1**. The cell parameters that reflect the dimensions of the individual layers of each structure ($a = 4.7569(3)$ Å, $c = 9.9147(5)$ Å, and $\beta = 95.292^\circ$ for **1** compared to $a = 4.6935(7)$ Å, $c = 11.1025(2)$ Å, $\beta = 94.724(3)^\circ$ for $Sb_2O(O_3PCH_2PO_3)$) are similar, with the difference in c is likely due to the constraints imposed by the $Sb_2O(O_3PCH_2PO_3)$ framework.

3.2. *Structure of* **2**, $NH_4(SbO)_3(CH_3PO_3)_2$

2 is constructed from three $[SbO_4E]$ trigonal bipyramids and two $[MePO_3]$ tetrahedra. The smallest rings are two unique Sb_2P 3-rings, joining to form a $[SbO_4E]$-based spiro-5 moiety (Fig. 4). These in turn combine to produce rings made of six oxygen-bridged Sb^{III} cations (Fig. 5). These star-shaped Sb_6 rings, similar to those found in the cetineite family of materials (2), are connected to each other through $[MePO_3]$ units (creating Sb_4P_2 rings in the process) from which arise nanotubes running in the [100] direction (Fig. 5). Opposite Sb^{III} centers in the Sb_6 *6-ring* are 7.012 Å apart on average, about the same distance as opposite T-atoms in a zeolitic *8-ring* (the Sb–O bond distance is about 0.4–0.5 Å longer than that of Si–O or Al–O). The number of four-coordinated Sb^{III}/P^{V} cation centers per cubic nanometer in **2** is 16.1, comparable to the Si^{IV}/Al^{III} tetrahedral-site (T-site) density of zeolites ($\sim$ 12–21). It should be emphasized, however, that the arrangement of the much larger O^{2-} anions in **2** (opposite anions are 5.339 Å apart, on average) gives the tubes very small openings, and porosity is precluded by the presence of charge-compensating NH_4^+ cations.

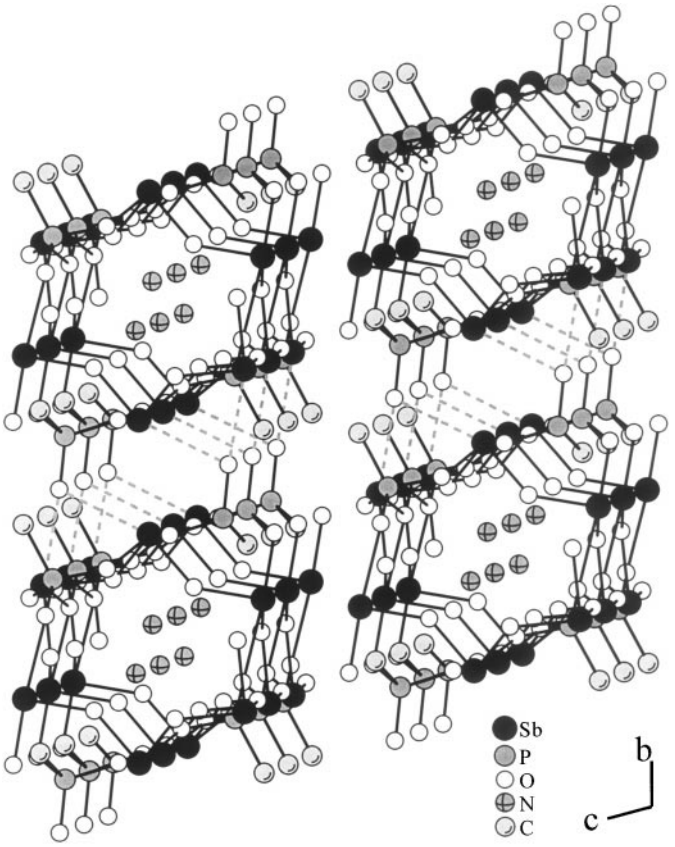

FIG. 5. The Sb_6 6-ring delimits channels in **2** running down the [100] direction. Methyl groups lie outside the tubes. Dashed lines indicate secondary Sb–O interactions ($2.7 < r_{Sb-O} < 3.1$ Å).

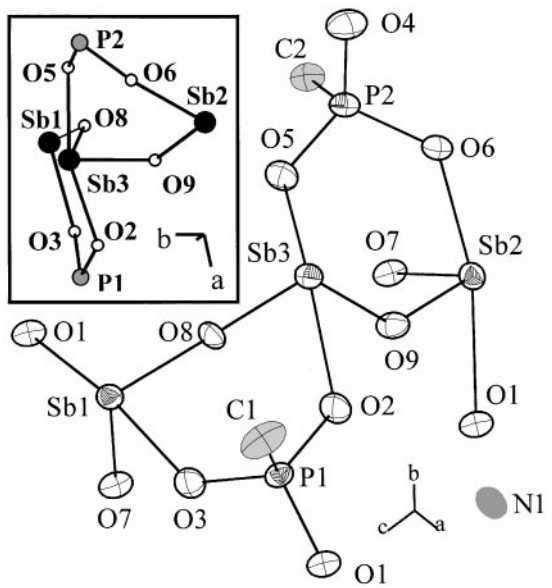

FIG. 4. Local coordination spheres of $NH_4(SbO)_3(CH_3PO_3)_2$ (**2**), illustrating the $[SbO_4E]$-based spiro-5 unit. The inset better shows the orientation of the rings with respect to one another. Thermal ellipsoids are given at 50% probability.

A notable feature of **2**, besides being part of a small, albeit growing, family of monophosphonates featuring channels [e.g., AlMePO-α and -β (20, 21), β-$Cu(CH_3PO_3)$ (22), and $Zn(O_3P)(CH_2)_2NH_2$ (23)], is that the overall structure is not a fully connected framework but rather a solid made of discrete nanotubes (Fig. 5). It is similar to reported tubular uranyl (24) and vanadium phenylphosphonates (25) in that terminal organic groups lie outside the channels rather than inside (as in the reported *framework* monophosphonates) (20–23). **2** is not appreciably soluble in water, simple alcohols, or acetone, probably due to bonding interactions between tubes, namely (i) hydrogen bonding between methyl groups (H(1B)---H(1B) = 2.843 Å, H(1B)---H(1C) = 2.577 Å) and between methyl and terminal P=O moieties (H(1A)---O(4)=2.715 Å, H(1C)---O(4) = 2.875 Å); and (ii) secondary Sb–O interactions with the P=O group (Sb(1)---O(4) = 2.764 Å, Sb(3)---O(4) = 2.912 Å). If these latter inter-

actions are depicted (Fig. 5, dashed lines), **2** can be viewed alternatively as rows of tubes comprising layers in the *ab* plane.

3.3. Thermal Behavior of *1* and *2*

2 is stable to 280°C in air, where it begins the following transformation: $NH_4(SbO)_3(CH_3PO_3)_2 \rightarrow Sb_2O(CH_3PO_3)_2 + NH_3 + \frac{1}{2}H_2O + \frac{1}{2}Sb_2O_3$, (or $\mathbf{2} \rightarrow \mathbf{1} + NH_3 + \frac{1}{2}H_2O + \frac{1}{2}Sb_2O_3$). Loss of NH_3 and H_2O is complete by 330°C (weight loss 4.0%, calcd 4.2%). Mass spectrometry confirms the evolution of both NH_3 and H_2O. The TGA was stopped at 360°C and the remaining sample was confirmed to be a mixture of **1** and Sb_2O_3 by powder diffraction, while elemental analysis showed no significant difference in the Sb/P ratio between the starting material (1.52, atom basis) and the product (1.48). If the TGA experiment is allowed to continue, the mixture is stable to 400°C in air, when it begins to lose 2.1% of its weight (calcd 2.4%, assuming a mixture of 1.0 **1**:0.5 Sb_2O_3, mole basis), and the transformation into $SbPO_4$ (confirmed by X-ray diffraction and elemental analysis) is complete by 460°C.

4. DISCUSSION

Open frameworks that contain 3-rings are of interest in part because silicates containing smaller rings tend to be more open (26). Since only one reported nanoporous aluminosilicate has 3-rings (27), the search for *tetrahedrally* connected open frameworks containing 3-rings has expanded to other systems, including the beryllo- (28, 29), litho- (30), and zincosilicates (31–33); beryllo- (34) and zincophosphates (35); and alumino- and gallogermanates (36). The longer T–O bond distances and smaller T–O–T bond angles of $[MO_4]$ tetrahedra (M = Be, Zn, Ga, Ge) are more amenable to 3-ring geometry than $[AlO_4]$, $[PO_4]$, or $[SiO_4]$ tetrahedra. It is not surprising then that the four-connected $[SbO_4E]$ *trigonal pyramids* can accommodate the constraints of the Sb_2P ring. Of more significance is the second example (5) of a $[SbO_4E]$-based spiro-5 unit in **2** since the tetrahedrally based spiro-5 is known in only a few of the 3-ring-containing open frameworks cited above (27, 29, 30, 32–34).

Whether the mechanisms to form **1** and **2** involve condensation of discrete molecular building units (MBUs) (37), chain-to-layer transformations (38), or other intermediates (e.g., $\mathbf{1} + NH_4^+ + SbO_2^- \rightarrow \mathbf{2}$, as suggested by the TGA) is, of course, unknown. Formally, at least, the synthesis of **2** can be written as a condensation of hypothetical MBUs:

$$NH_4[SbO(OH)_2]Sb[CH_3PO_2OH]_2 \rightarrow NH_4(SbO)_3(CH_3PO_3)_2 + 3H_2O$$

(the MBU could be the unit shown in Fig. 4, coupled to a NH_4^+ cation, where all terminal O centers are OH groups). It should be emphasized that the tubular material (**2**) is produced with greater selectivity over the layered material (**1**) in ethanol compared to ethylene glycol (39). In contrast, for both tubular phenylphosphonates it was suggested the high dielectric constant of water promotes the synthesis of the tubular material, since syntheses in nonaqueous solvents were unsuccessful (25, 40). In all three phosphonate systems, the introduction of a small cation favors a tubular material over a layered material. The small cation could also be necessary for formation of the $[SbO_4E]$ spiro-5 units: the unit is found in $NaSb_3O_2(PO_4)_2$, while the few reported antimony(III) phosphates/phosphonates/phosphites synthesized hydrothermally in the absence of cations (6, 41, 42) contain only even-membered rings (Sb_2P_2, Sb_3P_3, Sb_4P_4, …) or edge-sharing odd-membered rings. Certainly, more Sb_2P rings and $[SbO_4E]$-based spiro-5 motifs will be found, though it remains to be seen if the presence of these units will lead to *nanoporous* open antimony(III) phosphate/phosphonate frameworks.

ACKNOWLEDGMENTS

This work was supported by the UC Los Alamos National Laboratory under Award No. 9746-2-RPI and by the MRSEC Program of the National Science Foundation under Award No. DMR96-32716. B.A.A. thanks the Corning Foundation for a fellowship. We thank Dr. T. Loiseau for helpful discussions and the CNRS for providing a PICS grant to support collaboration between the Institut Lavoisier and the UCSB-MRL.

REFERENCES

1. J. B. Parise, *Science* **251,** 293 (1991).
2. C. Sabelli, I. Nakai, and S. Katsura, *Am. Mineral.* **73,** 398 (1988).
3. U. Simon, F. Schüth, S. Schunk, X. Wang, and F. Liebau, *Angew. Chem., Int. Ed. Engl.* **36,** 1121 (1997).
4. (a) S. Natarajan, M. P. Attfield, and A. K. Cheetham, *Angew. Chem., Int. Ed. Engl.* **36,** 978 (1997); (b) S. Natarajan and A. K. Cheetham, *J. Chem. Soc., Chem. Commun.* 1089 (1997); (c) S. Natarajan and A. K. Cheetham, *J. Solid. State Chem.* **134,** 207 (1997).
5. (a) B. A. Adair, G. D. Díaz de Delgado, J. M. Delgado, and A. K. Cheetham, *Angew. Chem., Int. Ed.* **39,** 745 (2000); (b) B. A. Adair, G. D. Díaz de Delgado, J. M. Delgado, and A. K. Cheetham. *J. Solid State Chem.* **151,** 21 (2000).
6. B. A. Adair, G. D. Díaz de Delgado, J. M. Delgado, and A. K. Cheetham, *Solid State Sci.* **2,** 119 (2000).
7. A. K. Cheetham, G. Férey, and T. Loiseau, *Angew. Chem., Int. Ed.* **38,** 3269 (1999).
8. A. Boultif and D. Louër, *J. Appl. Crystallogr.* **24,** 987 (1991).
9. A. D. Mighell, C. R. Hubbard, and J. K. Stalik. "NBS*AIDS80: A Fortran Program for Crystallographic Data Evaluation," Technical Note No. 1141. Natl. Bur. of Standards, Washington, DC, 1981. [NBS*AIDS83 is an expanded version of NBS*AIDS80]
10. A. Altomare, M. C. Burla, M. Camalli, B. Carrozzini, G. L. Cascarano, C. Giacovazzo, A. Guagliardi, A. G. G. Moliterni, G. Polidori, and R. Rizzi, *J. Appl. Crystallogr.* **32,** 339 (1999).
11. A. Altomare, M. C. Burla, G. Cascarano, C. Giacovazzo, A. Guagliardi, A. G. G. Moliterni, and G. Polidori, *J. Appl. Crystallogr.* **28,** 842 (1995).

12. A. Altomare, M. C. Burla, M. Camalli, G. L. Cascarano, C. Giacovazzo, A. Guagliardi, A. G. G. Moliterni, G. Polidori, and R. Spagna, *J. Appl. Crystallogr.* **32,** 115 (1999).
13. J. Rodriguez-Carvajal, "Collected Abstracts of Powder Diffraction Meeting," p. 127. Toulouse, France, 1990.
14. T. Roisnel and J. Rodriguez-Carvajal, "Abstracts of the 7th European Powder Diffraction Conference," p. 71. Barcelona, Spain, 2000.
15. R. A. Young and D. B. Wiles, *J. Appl. Crystallogr.* **15,** 430 (1982).
16. R. A. Young, "Proc. Egyptian 3rd Int. School Crystallogr.," p. 60. Cairo, Egypt, 1990.
17. G. M. Sheldrick, "SADABS User Guide." University of Göttingen, Göttingen, Germany, 1995.
18. G. M. Sheldrick, "SHELXL-97, A Program for Crystal Structure Determination." University of Göttingen, Göttingen, Germany, 1997.
19. $R(F) = \sum||F_o| - |F_c||/\sum|F_o|$ against 2350 reflections where $F > 4\sigma(F)$. $R_w(F^2) = \{\sum w(F_o^2 - F_c^2)^2/\sum w(F_o^2)^2\}^{1/2}$ against all 2751 unique reflections.
20. K. Maeda, Y. Kiyozumi, and F. Mizukami, *Angew. Chem., Int. Ed. Engl.* **33,** 2335 (1994).
21. K. Maeda, J. Akimoto, Y. Kiyozumi, and F. Mizukami, *Angew. Chem., Int. Ed. Engl.* **34,** 1199 (1995).
22. J. Le Bideau, C. Payen, P. Palvadeau, and B. Bujoli, *Inorg. Chem.* **33,** 4885 (1994).
23. S. Drumel, P. Janvier, D. Deniaud, and B. Bujoli, *Chem. Commun.* 1051 (1995).
24. D. M. Poojary, A. Cabeza, M. A. G. Aranda, S. Bruque, and A. Clearfield, *Inorg. Chem.* **35,** 1468 (1996).
25. G. Bonavia, R. C. Haushalter, C. J. O'Connor, C. Sangregorio, and J. Zubieta, *Chem. Commun.* 2187 (1998).
26. G. O. Brunner and W. M. Meier, *Nature* **337,** 146 (1989).
27. S. L. Lawton and W. L. Rohrbaugh, *Science* **247,** 1319 (1990).
28. S. Merlino, *Eur. J. Mineral.* **2,** 809 (1990).
29. G. Giuseppetti, F. Mazzi, C. Tadini, and E. Galli, *Neues Jb. Miner. Monat.* **7,** 307 (1991).
30. S. H. Park, P. Daniels, and H. Gier, *Microporous Mesoporous Mater.* **37,** 129 (2000).
31. M. J. Annen, M. E. Davis, J. B. Higgins, and J. L. Schlenker, *Chem. Commun.* 1175 (1991).
32. M. J. Annen and M. E. Davis, *Microporous Mater.* **1,** 57 (1993).
33. C. Röhrig and H. Gies, *Angew. Chem., Int. Ed. Engl.* **34,** 63 (1995).
34. F. Walter, *Eur. J. Mineral.* **4,** 1275 (1992).
35. W. T. A. Harrison, R. W. Broach, R. A. Bedard, T. E. Gier, X. Bu, and G. D. Stucky, *Chem. Mater.* **8,** 691 (1996).
36. X. Bu, P. Feng, and G. D. Stucky, *J. Am. Chem. Soc.* **120,** 11204 (1998).
37. G. Férey, *J. Fluor, Chem.* **27,** 187 (1995).
38. S. Oliver, A. Kuperman, and G. A. Ozin, *Angew. Chem., Int. Ed.* **37,** 46 (1998).
39. While a small amount of water is necessary to form the Sb–O–Sb bonds present in both structures, using water as a solvent gives antimony(III) oxide as a product starting from antimony(III) oxide, likely due to its low solubility, and starting from antimony(III) acetate, likely due to rapid hydrolysis.
40. D. Grohol and A. Clearfield, *J. Am. Chem. Soc.* **119,** 9301 (1997).
41. B. Kinberger, *Acta Chem. Scand.* **24,** 320 (1970).
42. J. Loub and H. Paulus, *Acta Crystallogr.* **27,** 1106 (1981).